PHYSICAL REVIEW B, VOLUME 63, 020502(R)

Magnetic twin boundaries and flux pinning in the antiferromagnetic superconductor $ErNi_2B_2C$

N. Saha,[1] R. Surdeanu,[2] M. Marchevsky,[3] G. J. Nieuwenhuys,[1] C. D. Dewhurst,[4] R. J. Wijngaarden,[2] D. McK. Paul,[5] and P. H. Kes[1]

[1]*Kamerlingh Onnes Laboratory, Leiden University, POB 9504 Leiden, The Netherlands*

[2]*Division of Physics and Astronomy, Vrije Universiteit, De Boelelaan 1081, 1081HV Amsterdam, The Netherlands*

[3]*NEC Research Institute, 4 Independence Way, Princeton, New Jersey 08540*

[4]*Institut Laue-Langevin, 6 rue Jules Horowitz, BP 156-38042 Grenoble, France*

[5]*Department of Physics, University of Warwick, Coventry CV4 7AL, United Kingdom*

(Received 20 September 2000; published 20 December 2000)

We show that in the antiferromagnetic superconductor $ErNi_2B_2C$, the increase in flux pinning below T_N coincides with the appearance of twin boundaries between antiferromagnetic domains. The pinning mechanism is provided by a ferromagnetic spin component localized at the twin boundaries parallel to the crystallographic *c* axis.

DOI: 10.1103/PhysRevB.63.020502 PACS number(s): 74.70.Dd, 74.60.Ge, 74.60.Jg

The study of the mixed state of antiferromagnetic superconductors has made a remarkable revival since the discovery of the $(R)Ni_2B_2C$, where R = rare earth (RNBC).[1,2] Coexistence of antiferromagnetism and superconductivity was known to exist in $(R)Rh_4B_4$ and $(R)Mo_6(S/Se)_8$ with the exception of $ErRh_4B_4$ and $HoMo_6S_8$, but the value of the Néel temperature (T_N) is typically 2 K or less[3] and the superconducting transition temperatures (T_c) are much larger. However, RNBC compounds have a higher T_N and a T_c which is comparable, and this provides the opportunity to study the influence of long-range antiferromagnetic (AF) order on superconductivity. Hall-probe-array measurements on $HoNi_2B_2C$ (Ref. 4) show that bulk pinning is weak both in the *c*-axis spiral AF state ($T>6$ K) and the low-temperature commensurate AF phase ($T<5$ K) but that the pinning is much stronger in the intermediate ($5\ \mathrm{K}<T<6$ K) incommensurate AF phase. Similarly, in $ErNi_2B_2C$,[5] bulk pinning is weak in the paramagnetic phase between T_N (=6 K) and T_c (=10.5 K) and much stronger below T_N where the material magnetically orders into an incommensurate AF phase with a transversely polarized spin-density wave along the *a* axis with wave vector (0.553,0,0),[6] and the magnetic Er^{3+} moments parallel to (0,1,0). A weak ferromagnetically ordered component appears in this compound below T_{wfm} =2.5 K (Refs. 7 and 8) and is accompanied by a further increase of the bulk pinning.[9] In Refs. 4 and 5 it is suggested that the enhanced flux pinning is related to the incommensurability of the magnetic order and in Ref. 9 the further increase below T_{wfm} is speculated to be due to strong local-pair breaking by the ferromagnetism at the domain walls between differently oriented AF domains. Such AF twinning is quite common in R compounds.[10] In this paper we will further address the nature of flux pinning in the AF phase of $ErNi_2B_2C$.

In order to explore the underlying mechanism of flux pinning in these magnetic superconductors in general and in $ErNi_2B_2C$ in particular, we have performed Bitter decoration, magneto-optical and scanning Hall-probe experiments on single crystals of $ErNi_2B_2C$ in both the paramagnetic and AF phases. These experiments provide clear evidence for the formation of domain walls and the interaction of these walls with the vortex lattice (VL). The features of the VL observed in the AF phase are very similar to those observed in strongly twinned single crystals of $YBa_2Cu_3O_7$ (YBCO).[12,13] In addition, a field modulation across the domain wall is detected which clearly reveals weak local ferromagnetism. The weak ferromagnetism sets in immediately below T_N and therefore we think that this is the mechanism for the enhancement of flux pinning below the AF transition. The further increase below T_{wfm} as observed by Gammel *et al.*[9] requires an additional mechanism which has not yet been explored.

The experiments which are described here were performed on single crystals prepared using a high-temperature flux method. The crystals were platelets with the *c* axis normal to the platelet surface and typical sample sizes are 700 by 600 μm and 80 μm thick along the *c* axis. The orientation of the crystal was determined using Laue diffraction and the published c/a ratio of $ErNi_2B_2C$.[6] The sample was characterized using electron probe microanalysis (EPMA) and atomic force microscopy. It is chemically uniform and mechanically smooth. All experiments were done on the same single crystal. The surface was cleaned between successive decorations using rf-plasma etching. The $ErNi_2B_2C$ crystal has a T_c=10.5 K. Typical values of low-temperature penetration depth λ are 700 Å and coherence length $\xi \approx 150$ Å .[11] Three types of experiments were carried out on these samples. Bitter decoration experiments were performed after field cooling (FC) below and above T_N, scanning Hall-probe experiments after FC at 5.2 K and magneto-optic experiments both FC and zero-field cooled (ZFC) above and below T_N. Due to radiation heating the actual decoration temperature is slightly (<1.5 K) higher than the preset temperature. In this paper the temperature referred to is the estimated actual temperature of the sample during decoration.

A typical decoration picture on $ErNi_2B_2C$ (5 K) is shown in Fig. 1 for an applied field of 6 mT. Clearly visible are stripes at right angles to each other directed along [110] and

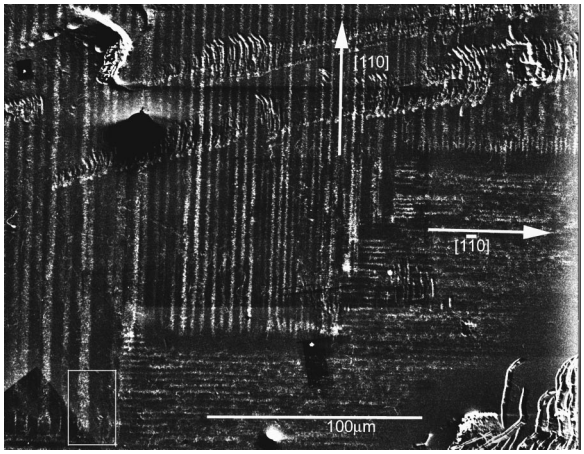

FIG. 1. A decoration picture of $ErNi_2B_2C$ (field cooled in 6 mT to 5 K). The separation between the stripes is approximately 3–10 μm along [110] and [1$\bar{1}$0]. They continue without deviation across surface steps.

[1$\bar{1}$0]. These stripes continue without deviation across large (a few micron) surface steps. This indicates that the origin of these linelike patterns is a bulk and not a surface effect. The distances between the stripes in all decorations below 6 K ranges between 3 and 10 μm. An enlargement of the marked area is shown in [Fig. 2(a)]. It is seen that the stripes consist of hexagonal vortex arrangements with one of the close-packed directions along [110] or [1$\bar{1}$0]. Square vortex arrangements are observed in the regions where two stripes meet at right angles. These observations are very reminiscent to the vortex configurations in twinned YBCO (Ref. 13) where vortices line up along the twin boundaries. The distance between the vortices inside the stripes is governed by the applied field. A study of the autocorrelation function of the VL in wide stripes, Fig. 2(c) shows that the translational correlation length is about 3 to 4 lattice spacings in all directions. In the areas between the stripes occasionally faint images of the VL are visible. For different FC experiments the line structure at the same sample site can change from [110] to [1$\bar{1}$0] or vice versa. There were no essential differences between FC experiments at 3 or 5 K. Our experimental setup does not allow us to go below $T_{wfm} \approx 2.5$ K. The decoration experiments done above 6 K do not show the stripes, in contrast a conventional hexagonal VL was observed with a correlation length of 3–4 lattice spacing and with the principal axis along [110] or [1$\bar{1}$0]. Such a VL orientation is in agreement with the predictions of Kogan *et al.*[14] The fact that the stripes disappear above 6 K implies that their existence is related to the AF transition.

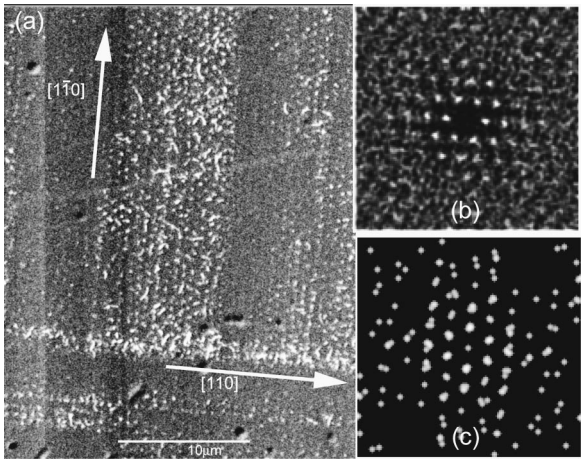

FIG. 2. (a) Enlargement of the vortex lattice in the marked area in Fig. 1 after field cooling in 6 mT to 5 K. (b) Structure factor shows that the vortex lattice is hexagonal with orientation along [110] and [1$\bar{1}$0]. (c) The two-dimensional autocorrelation function shows that translational correlation of the lattice exists over 3–4 lattice spacing.

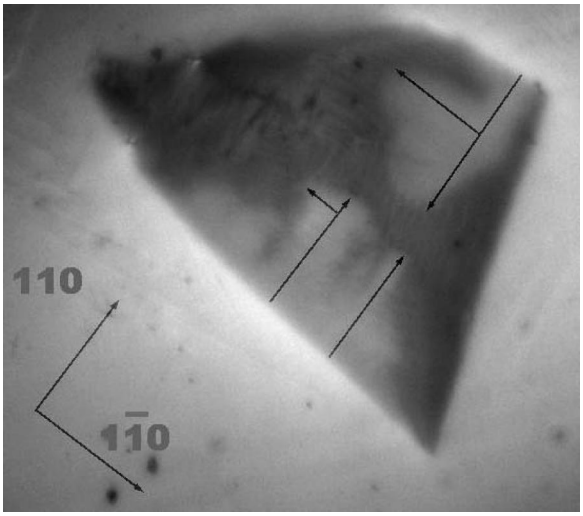

FIG. 3. Magneto-optical observation of flux penetration into $ErNi_2B_2C$ at 2 K. The sample was zero-field cooled to 2 K, the field was cycled to 45 mT and thereafter back to zero. The above picture was taken at 20 mT in increasing field.

The observation of line patterns reminiscent to the twin boundaries in YBCO points to the formation of domains coincident with the antiferromagnetic phase transition. As has been shown by Detlefs *et al.*[15] the crystal lattice of $ErNi_2B_2C$ undergoes a tetragonal ($T > 6$ K) to orthorhombic ($T < 6$ K) distortion at the onset of long-range antiferromagnetic order due to magneto-elastic coupling. In order to minimize strains the crystal lattice breaks up into domains with domain walls parallel to the *c* axis and [110] or [1$\bar{1}$0], on either side of which the direction of the *a* and *b* axes are interchanged.

In order to further confirm that these domain walls are related to the linelike patterns and to explore their effect on the pinning of the VL, magneto-optical experiments were carried out. The sample was ZFC to $T < T_c$ and the field was cycled from zero to 40 mT and back to zero. The resulting images were recorded. The experiments were repeated at 2, 4.2, 5.5, 6, 7, and 7.5 K. Distinctly different features were only observed below and above 6 K. There was no noticeable difference in flux penetration behavior at 2 K and above.

Figure 3 shows the nature of flux penetration into $ErNi_2B_2C$ at 2 K. Such images are typical for the behavior below T_N. It is seen that the flux penetrates very inhomoge-

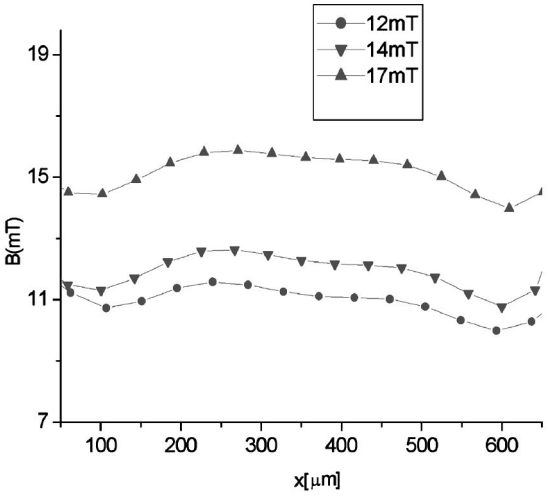

FIG. 4. The dome shaped flux profile deduced from magneto-optics at 7 K showing the absence of bulk pinning in the paramagnetic phase. Sample edges are at $x \approx 0$ μm and 700 μm.

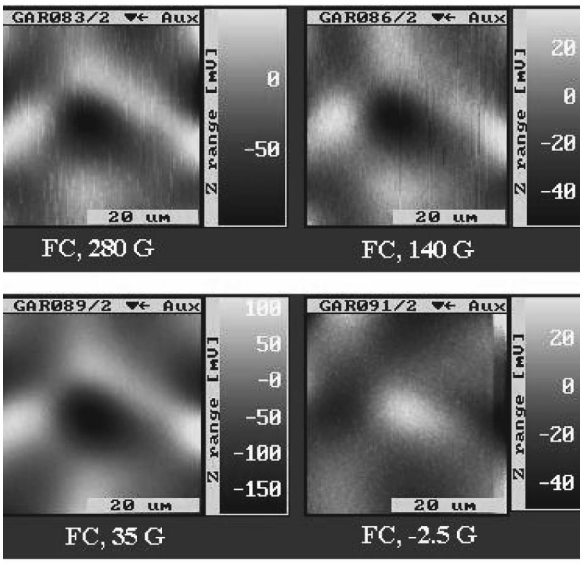

FIG. 5. Scanning Hall probe microscope images across a meeting point of two perpendicular stripes at 5.2 K and various applied fields. The size of the scanned region is approximately 40 by 40 μm. The background field has been subtracted. The field calibration is 900 V/T yielding a typical field modulation averaged over the size of the SHP of 1 mT. Note the black-white reversal upon zero-field crossing.

neously in the form of bubbles and finger shaped flux fronts. These observations are globally similar to the flux penetration in 2H-$NbSe_2$,[16] but there is a distinct difference in that there are two preferential directions of flux penetration corresponding to the directions of the stripe structures seen in the Bitter decoration. The directions of flux penetrations are indicated by the black arrows in Fig. 3. It means that flux lines easily penetrate along the domain walls and that in addition there are strong screening currents along the domain walls which drive the vortices into the areas in between. This kind of flux penetration behavior is very similar to that seen in twinned single crystals of YBCO,[17,18] indicating that the domain walls act as planar pinning centers which promote vortex channeling along them. In contrast, above 6 K, the flux penetrates uniformly yielding a flux profile which is dome shaped. A typical example at 7 K is shown in Fig. 4. The dome shaped flux profile is caused by strong screening currents at the edges of the sample due to its platelet geometry in combination with absence of bulk pinning.[19] An estimate of the edge current density J_e is obtained from the measured value of the first penetration field H_p (12 mT at 4.2 K) and the expressions[19] $H_p = H_{c1}\sqrt{d/W}$ and $J_e = 2H_{c1}/d$, where H_{c1} is the lower critical field, d is the sample thickness, and W is the sample width. The result is $J_e = 9 \times 10^8$ A/m^2. Information about the strength of the bulk pinning is deduced from the slope of the profile at the bubble front. The result at 4.2 K is $J_c \approx 7 \times 10^8$ A/m^2. Similar observations have been made with Hall-probe arrays by Dewhurst *et al.*[5] who concluded in agreement with our findings that bulk pinning is comparable to the geometrical barrier in the AF phase while in the paramagnetic phase bulk pinning is negligibly small.

We now turn to the questions why the line pattern is observed below 6 K and what the actual pinning mechanism in the AF phase is. The fact that we do not observe vortices in the regions between the stripes or occasionally only a faint image, means preferential deposition of the nickel particles takes place at and around the location of the domain walls. In order to explore this further we undertook scanning Hall probe experiments after cooling down the sample in different fields to a temperature of 5.2 K as shown in Fig. 5.

In analyzing the images it should be known that the size of the scanning Hall probe (SHP) is 1 by 1 μm, the distance to the sample surface is around 0.5 μm, the field calibration is 900 V/T at 5.2 K, and that only the field modulation is shown after subtraction of the applied background field. Figure 5 shows that across a domain wall the field variation is around 1 mT. The actual field variation at the domain wall is expected to be larger, but it cannot be precisely detected due to the finite size of the SHP. It is further seen that the amplitude of the modulation is independent of the applied field and that upon changing the polarity of the applied field the overall image reverses sign.

This is convincing evidence for local ferromagnetism at the domain walls with an internal field component parallel to the c axis. The resulting magnetic field above the sample will thus have strong gradients at the domain walls which attract the nickel particles during decoration. The stripes in Fig. 1 therefore show the positions of the domain walls. On the other hand, SHP probes the field modulation and this has twice the periodicity of the domain walls. Thus the distance between the brighter areas in Fig. 5 should approximately be twice as large as the distance between the stripes in Fig. 1, which is indeed the case.

The origin of the local ferromagnetism can be explained as follows. At the domain walls both the crystallographic orientation and the orientation of the Er moments change by 90°. This gives rise to a region of magnetic frustration which we believe leads to local canting of the Er moments away from the basal (a-b) plane. Depending on the amount of

canting this results in a strong local magnetic field. We estimate that this local field can be 300 mT if we assume a canting of the Er^{3+} moments by an angle of 10° out of the ab plane and a width of the domain wall of a few crystal lattice parameters. We further note that Mossbauer spectroscopy[20] has demonstrated the existence of a net c-axis component of the Er^{3+} moments in the AF phase. Since the experiments in Ref. 20 were done on polycrystalline samples, these results were not decisive as to the location of the canted moments. Our work shows that they coincide with the boundaries between the AF domains.

It is obvious that strong local internal fields at the domain walls will severely suppress superconductivity. In addition, it may also be the reason for the drop in H_{c2} below T_N in the phase diagram of $ErNi_2B_2C$. The domain walls will therefore act as strong planar pinning centers, very similar to the twin boundaries in YBCO,[21] except that the pinning mechanism will be δT_c pinning rather than the $\delta\kappa$ pinning suggested by Gammel *et al.*[9] We believe that the domain-wall related ferromagnetism provides a plausible explanation for the sudden appearance of flux pinning below T_N. Since the onset of bulk pinning coincides with the appearance of a transverse spin-wave modulation of Er moments, one might suspect that coupling of the VL to the spin-wave structure could be a source of flux pinning. However, the modulation will be smeared out over the relevant length scales of the VL which will make this pinning mechanism less effective. We finally note that it would be interesting to study the interplay of internal magnetism and the VL when the formation of domain walls could be suppressed.

In conclusion, we have performed Bitter decoration, magneto-optical and scanning Hall-probe measurements in the mixed state of the antiferromagnetic superconductor $ErNi_2B_2C$. The enhancement of flux pinning in the antiferromagnetic phase is caused by the formation of magnetic twin boundaries at which a local variation of the internal magnetic field is related to the ferromagnetic component of the Er^{3+} moments along the crystallographic c axis.

The authors wish to thank Professor Aronson from the University of Michigan and Professor Ramakrishnan from Tata Institute, Bombay for helpful discussions. Technical assistance from Marcel Hesselberth, Ton Gortenmulder, and Ruud Hendrikx was of great help. This work was part of the research program of FOM, the ''Stichting voor Fundamental Onderzoek der Materie,'' which was financially supported by ''NWO.''

[1] C. Mazumdar *et al.*, Solid State Commun. **87**, 413 (1993).
[2] R. Nagarajan *et al.*, Phys. Rev. Lett. **72**, 274 (1994).
[3] D. C. Johnston *et al.*, *Superconductivity in Ternary Compounds, Vol. II*, edited by M. B. Maple and O. Fisher (Springer, Berlin, 1982), p. 11.
[4] C. D. Dewhurst, R. A. Doyle, E. Zeldov, and D. McK. Paul, Phys. Rev. Lett. **82**, 827 (1999).
[5] C. D. Dewhurst, S. S. James, R. A. Doyle, Y. Paltiel, E. Zeldov, and D. McK. Paul (unpublished).
[6] J. Lynn *et al.*, Phys. Rev. B **55**, 6584 (1997).
[7] B. K. Cho, P. C. Canfield, L. L. Miller, D. C. Johnston, W. P. Beyermann, and A. Yatskar, Phys. Rev. B **52**, 3684 (1995).
[8] H. Kawano, H. Takeya, H. Yoshizawa, and K. Kadowaki, J. Phys. Chem. Solids **60**, 1053 (1999).
[9] P. L. Gammel *et al.*, Phys. Rev. Lett. **84**, 2497 (2000).
[10] P. Morin and D. Schmitt, in *Ferromagnetic Materials*, edited by K. H. J. Buschow and E. P. Wohlfarth (North-Holland, Amsterdam, 1990), Vol. 5.
[11] P. L. Gammel *et al.*, Phys. Rev. Lett. **82**, 1756 (1999).
[12] L. Ya. Vinnikov *et al.*, Solid State Commun. **67**, 412 (1988).
[13] G. J. Dolan, G. V. Chandrashekhar, T. R. Dinger, C. Feild, and F. Holtzberg, Phys. Rev. Lett. **62**, 827 (1989).
[14] V. G. Kogan *et al.*, Phys. Rev. B **54**, 12 386 (1996).
[15] C. Detlefs *et al.*, Phys. Rev. B **56**, 7843 (1997).
[16] M. Marchevsky, L. A. Gurevich, P. H. Kes, and J. Aarts, Phys. Rev. Lett. **75**, 2400 (1995).
[17] Rinke J. Wijngaarden, R. Griessen, J. Fendrich, and W. K. Kwok, Phys. Rev. B **55**, 3268 (1997).
[18] C. A. Durán, P. L. Gammel, D. J. Bishop, J. P. Rice, and D. M. Ginsberg, Phys. Rev. Lett. **74**, 3712 (1995).
[19] E. Zeldov *et al.*, Phys. Rev. Lett. **73**, 1428 (1994).
[20] P. Bonville *et al.*, Z. Phys. B: Condens. Matter **101**, 511 (1996).
[21] P. H. Kes *et al.*, Cryogenics **29**, 228 (1989).